

# Letters

## Comments on "Revisiting Characteristic Impedance and Its Definition of Microstrip Line with a Self-Calibrated 3-D MoM Scheme"

James C. Rautio

### I. BACKGROUND

Characteristic impedance ( $Z_0$ ) is well understood for lossless homogeneous transmission lines. These include, for example, coaxial cable, stripline, and rectangular waveguide. (Note that while rectangular waveguide is dispersive and non-TEM, impedance is uniquely defined because it is homogeneous.) In these cases, for a given mode, propagating in a given direction, at a given frequency, the ratio of transverse  $E$  to transverse  $H$  is constant everywhere. The value of this ratio is the characteristic impedance of the line. An equivalent-circuit theory voltage and current can then be derived, purely from the transverse fields (even for non-TEM modes) which corresponds to that impedance.

However, the fields of an inhomogeneous transmission line exist in multiple regions of different dielectric. The ratio of transverse  $E$  to transverse  $H$ , and thus the impedance of the wave propagating in the guide, is a function of location in the cross section of the guide. There then result a multitude of nonunique definitions of characteristic impedance for inhomogeneous transmission lines, generally based on various definitions of voltage, current, and power. These definitions can be viewed as a weighted average of the actual wave impedance (i.e., transverse  $E$  over transverse  $H$ ) as it varies throughout the cross section of the guide.

In one well-known investigation of  $Z_0$  with specific attention to the inhomogeneous nature of the problem [1], Jansen explored three definitions with the general conclusion that a current-power definition provides a value for  $Z_0$  that is most consistent with physical reality. The problem is important because the various definitions of  $Z_0$  yield values covering a 20% range.

More recently, this author proposed a definition of  $Z_0$  [2] that considers the terminal voltages and currents of a finite length of inhomogeneous transmission line. The non-TEM line's terminal behavior is used to determine the  $Z_0$  of an equivalent TEM transmission line, thus the name, "TEM equivalent characteristic impedance." It is this definition of  $Z_0$  which is used in the Sonnet electromagnetic analysis.<sup>1</sup> Since the definition of  $Z_0$  depends on the three-dimensional (3-D) fields of a finite length of transmission line, rather than the two-dimensional (2-D) cross-sectional fields of an infinite length of line, it is called a 3-D  $Z_0$  definition.

Following the publication of [2], a similar definition of  $Z_0$  [3] was brought to this author's attention. Here,  $Z_0$  is defined by means of an analysis of a junction between a stripline and an otherwise identical, but homogeneous, shielded microstrip (i.e., an air substrate). The fields of the step junction are written as a sum of the modes of each transmission-line medium with the amplitudes of

Manuscript received February 25, 1998; revised October 1, 1998.

The author is with Sonnet Software, Inc., Liverpool, NY 13088 USA (e-mail: rautio@sonnetusa.com).

Publisher Item Identifier S 0018-9480(99)00395-6.

<sup>1</sup>J. C. Rautio, *The Em Users Manual*, Sonnet Software, Liverpool, NY 13088.

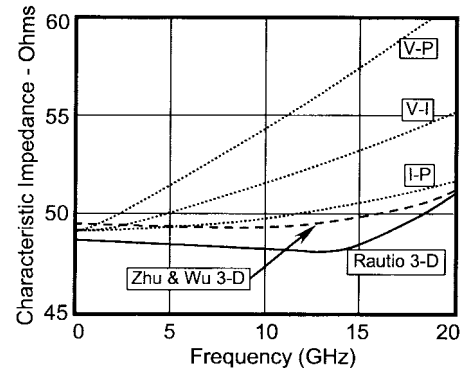


Fig. 1. The characteristic impedance of a microstrip line according to various definitions. The  $V-P$ ,  $V-I$ , and  $I-P$  curves are from [1]. The Rautio 3-D curve is from [2] and the Zhu and Wu curve is from the above paper<sup>2</sup>. The transmission line is 0.635-mm-wide on a 0.635-mm substrate with an epsilon relative of 9.7.

each mode determined by matching tangential boundary conditions at the junction. The  $Z_0$  of the fundamental mode of the microstrip is then written in terms of the well-defined  $Z_0$  of the rectangular stripline.

Most recently, the above paper<sup>2</sup> proposed a means of determining the TEM equivalent  $Z_0$ , which is similar to the technique described by this author in [2]. While [2] assumes the port discontinuity to be a single shunt capacitance, the port discontinuity assumed by Zhu and Wu is more general. Their key figure is repeated here as Fig. 1. The transmission line under consideration has a width of 0.635 mm, with a substrate 0.635-mm-thick with a relative dielectric constant of 9.7. Zero thickness and zero loss are assumed. Although incidental to this letter, it is interesting to note that Zhu and Wu show the same nonmonotonic dispersion in  $Z_0$  that was first reported in [2].

The authors of the above paper<sup>2</sup> suggest that the 2% difference is due to error in Rautio's analysis. In order to check this hypothesis, an error analysis must be performed. The purpose of this paper is to communicate the results of just such an error analysis for Rautio's analysis.

### II. CHARACTERIZATION OF SPECIFIC ERROR SOURCES

The sources of error we consider are as follows ( $N_W$  is the number of cells across the line width,  $N_L$  is the number of cells per wavelength along the length of the line).

- 1)  $N_W$  error: This is error due to subsection width. When  $N_L$  is large, this error shows an extremely well-behaved convergence behavior. Specifically, when  $N_W$  is doubled,  $N_W$  error is cut in half. This error is removed by evaluating the error for  $N_W = 128$  and  $N_W = 256$ . A high-accuracy extrapolation to  $N_W = \text{infinity}$  is simple [7], [8]. The final  $N_W$  error is estimated to be half the change in  $Z_0$  seen between the two cases. Due to the well-behaved convergence, the actual  $N_W$  error is likely to be much less.
- 2)  $2A$  error: In evaluating the TEM equivalent  $Z_0$ , Sonnet calculates two transmission lines, the first  $A$  units long and the

<sup>2</sup>L. Zhu and K. Wu, *IEEE Microwave Guided Wave Lett.*, vol. 4, no. 2, pp. 87-89, Feb. 1998.

TABLE I  
CONVERGED VALUE OF  $Z_0$  FOR  $A = 2.54$  mm

Freq. (GHz)	$Z_0$ (Ohms)	Nw Error	2A Error	2B Error	Total Error
2.0	48.997	0.022%	0.552%	0.000%	0.574%
4.0	49.005	0.022%	0.373%	0.000%	0.395%
6.0	49.026	0.022%	0.134%	0.000%	0.156%
8.0	49.076	0.022%	0.079%	0.001%	0.101%
10.0	49.178	0.022%	0.147%	0.001%	0.170%
12.0	49.367	0.022%	0.136%	0.002%	0.160%
14.0	49.700	0.022%	0.171%	0.005%	0.198%
16.0	50.278	0.022%	0.164%	0.012%	0.198%
18.0	51.325	0.022%	0.255%	0.042%	0.318%
20.0	53.609	0.021%	1.181%	0.248%	1.450%

second  $A/2$  units long. The  $Z_0$  calculation assumes that there is only one propagating mode on the transmission line. If this is true, then the evaluation of  $Z_0$  is independent of the actual value of  $A$ . Thus, to check for this error source, we first evaluate  $Z_0$  using a line of length  $A$  (and  $A/2$ ), then again using a line of length  $2A$  (and  $A$ ). Any change in  $Z_0$  between the two cases is attributed to undesired coupling between the input and output ports of one of the lines. At high frequency, this is usually due to higher order propagating modes or box resonances. At low frequencies with small values of  $A$ , this is due to fringing field interaction between the two ports.  $2A$  error is estimated to be equal to the change in  $Z_0$  between the two cases.

- 3)  $2B$  error: Sidewalls are a required part of the Sonnet analysis. The dimension of the substrate transverse to the transmission lines is  $B$ . The presence of sidewalls at  $B/2$  to either side of the transmission line lowers the calculated  $Z_0$ . If we double  $B$ , the change in  $Z_0$  reflects the amount of influence the sidewalls have on characteristic impedance.  $2B$  error is subtracted from the final result and the error is estimated to be half the change in  $Z_0$  between the two cases. Because  $2B$  error converges rapidly, the actual error is likely to be much less.
- 4)  $N_L$  error: Subsection length has little effect on  $Z_0$ . Even so,  $N_L$  error was explicitly evaluated. With  $N_W = 256$ , we evaluated cases for  $N_L$  at about 300 and about 600 per wavelength at 20 GHz (128 and 256 per 2.54 mm).  $N_L$  error was estimated by taking the difference in  $Z_0$  resulting from the two cases. It was found to range from 0.0002% error at 2 GHz to 0.01% at 20 GHz. This error source received no further consideration.
- 5) *Cell-merging error*: The Sonnet analysis merges cells into larger subsections, leaving narrow subsections on the edge and wider subsections in the center. While substantially reducing the size of the matrix to be solved, this technique also increases error. To quantify the increase in error, we solved a line meshed 16 cells across and 128 cells long, first with the merged meshing and then without. Differences in  $Z_0$  between the two analyzes range from 0.004% at 2 GHz to 0.07% at 20 GHz. This error source received no further consideration.
- 6) *Total error*: Total error is taken as a straight sum of all errors. Root sum squared (RSS) error was not used so as to present a worst-case scenario.

The results are in the accompanying tables. Table I shows the calculated  $Z_0$  for  $A = 2.54$  mm and  $B = 20.32$  mm. Note that  $2A$  error increases rapidly at high frequency. This is probably due to an undesired mode or box resonance. The increase in  $2A$  error at low frequency is most likely due to fringing field interaction between the two ports of the  $A/2$ -length transmission line.

Table II shows the results for a similar analysis with  $A = 5.08$  mm. Note the complete absence of  $2A$  error at low frequency, supporting

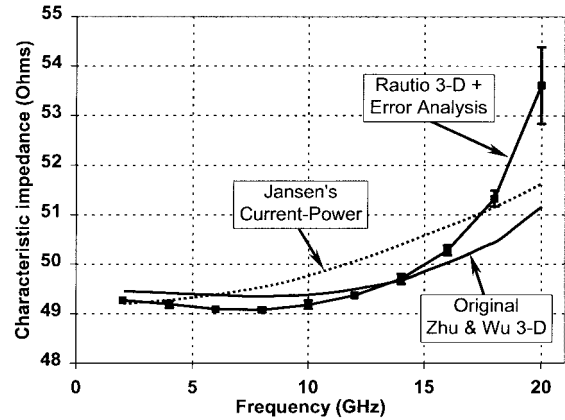


Fig. 2. Calculated TEM equivalent characteristic impedance for a 0.635-mm-wide line on a 0.635-mm substrate of epsilon relative 9.7. The error bars indicate the sum of the  $N_W$  error,  $2A$  error, and  $2B$  error. Zhu and Wu's original curve and Jansen's current-power curve are presented for reference.

TABLE II  
CONVERGED VALUE OF  $Z_0$  FOR  $A = 5.08$  mm

Freq. (GHz)	$Z_0$ (Ohms)	Nw Error	2A Error	2B Error	Total Error
2.0	49.268	0.022%	0.014%	0.001%	0.037%
4.0	49.188	0.023%	0.118%	0.002%	0.143%
6.0	49.092	0.025%	0.055%	0.004%	0.084%
8.0	49.038	0.028%	1.184%	0.007%	1.219%
10.0	49.106	0.033%	5.918%	0.012%	5.963%

the fringing field-interaction hypothesis suggested above. However,  $2A$  error increases at high frequency, as with the  $A = 2.54$  mm case mentioned above.

Fig. 2 plots the  $Z_0$  estimate from either Table I or II depending on which estimate has the smallest error. The estimated error for each data point is indicated with error bars. The reader should be cautioned that the error estimates are valid only if all error sources have been properly considered. Data above 16 GHz should especially be considered tentative due to the large effect  $2A$  error has demonstrated.

In comparison with the original results obtained by this author (Fig. 1), we see that the originally calculated  $Z_0$  is about 1.5% low. After investigating the original analysis, it was found that it used a  $B$  dimension of 5 mm, as compared with the current 20 mm. Repeating the analysis with a  $B$  dimension of 5 mm confirms that the 1.5% error in the original analysis is caused by the close proximity of the sidewalls, i.e.,  $2B$  error.

For all analyses, a perfectly conducting top cover is in place 6 mm above the surface of the substrate. Cell length is 2.54 mm/128 cells and  $B = 20.32$  mm. For the  $N_W = 256$  case, the cell width is 20.32 mm/8096 cells. For the  $N_W = 128$  case, 4096 cells are used along the same  $B$  dimension. In the course of all the analyzes, the largest analysis requires fast Fourier transform (FFT) of  $1024 \times 16382$  taking about 10 min per frequency. Most analyzes are under 1 min. The processor is a 266-MHz Pentium. Memory requirements are under 40 Mbytes. About twice as much effort was required to prepare the error analysis as was required to simply evaluate the value of  $Z_0$ .

### III. COMPARISON OF RESULTS

As we can see in Fig. 2, after characterization (and removal, where possible) of all error sources, the new evaluation of  $Z_0$  is within 1% of the above paper's<sup>2</sup> results over most of the frequency range. However, no error analysis or convergence analysis has been reported for the above paper's<sup>2</sup> results. Since the authors of the above paper<sup>2</sup>

specify the cell size used for their analysis, we can estimate expected error due to cell size.

As has been detailed in [4]–[8], the error in  $Z_0$  when using rooftop basis functions is closely upper bounded by the expression:

$$Z_0 \text{ Error}(\%) \leq 16/N_W \quad (1)$$

where

$N_W$  = Number of cells across the width of the line.

Since the  $Z_0$  error due to  $N_W$  is caused by the difference between the analyzed current distribution and the true current distribution, we expect this expression to be true for both open and shielded environment analyzes using rooftop expansion and testing functions. (Note that this inequality does not include error due to other error sources.)

Since the results of the above paper<sup>2</sup> use  $N_W = 5$ , we expect error of about 4%. In practice,  $N_W$  error (when acting alone) has always been found to result in estimates of  $Z_0$  which are high. Thus, we expect a convergence analysis with respect to  $N_W$  on the results of the above paper<sup>2</sup> to decrease  $Z_0$  by about 4% ( $2 \Omega$ ). While the above paper's<sup>2</sup> data as plotted appears to match the current–power definition well, if the expected  $N_W$  error actually exists, the  $N_W$  converged result is moved down off the bottom of the chart in Fig. 2.

We are left with the following three possibilities.

- 1) There are additional error sources in the Sonnet analysis, which have not been properly considered.
- 2) There are multiple error sources in the above paper's<sup>2</sup> analysis, which tend to cancel [6], yielding the reported results.
- 3) Error sources have been removed from the above paper's<sup>2</sup> analysis in a manner which is not reported within it.

We welcome specific suggestions as to potential error sources for possibility 1). To test possibility 2), we suggest performing an error analysis for the above paper's<sup>2</sup> analysis with concentration on  $N_W$  error and  $N_L$  error, the two error sources most likely to be canceling ( $N_L$  in the above paper<sup>2</sup> is nine cells/wavelength at 20 GHz).

We also note that because both microstrip current and power are unique and should be identical to the equivalent TEM-line circuit-theory quantities, we would expect Jansen's current–power  $Z_0$  result in [1] to be identical to our TEM equivalent  $Z_0$  result. However, because an error analysis of [1] has never been published, it is entirely possible that the differences between our TEM equivalent  $Z_0$  and Jansen's current–power  $Z_0$  are insignificant (see Fig. 2).

#### IV. POTENTIAL FOR MEASUREMENT

Microstrip characteristic impedance was measured by Getsinger [9]. While the measurements have relatively large error, in general, they support the TEM equivalent  $Z_0$ . The deembedding algorithm [2] from which the TEM equivalent definition is derived allows only pure shunt capacitance at the port discontinuities. For the Sonnet analysis, no further sophistication of the port is required as the Sonnet port discontinuity has no series inductance component. However, this restriction is not appropriate for measurement, thus precluding this deembedding algorithm from being used, at least without modification, for precise measurement of  $Z_0$ .

However, the introduction of Zhu and Wu's technique<sup>2</sup>, wherein the port discontinuity is more general, now suggests possible application to measurement. If this is done, precision measurement of  $Z_0$  becomes possible. This then permits not only an experimental

validation of the TEM equivalent definition, but also permits both the measurement and analysis of microwave circuits to be tied to the same  $Z_0$  standard, thus allowing, for the first time, direct and absolute comparison of measured microstrip data with calculated data. With the increasing accuracy of both measurements and analysis, using the same definition of  $Z_0$  for both is becoming important.

#### REFERENCES

- [1] R. J. Jansen and N. H. L. Koster, "New aspects concerning the definition of microstrip characteristic impedance as a function of frequency," in *IEEE MTT-S Int. Microwave Symp. Dig.*, 1982, pp. 305–307.
- [2] J. C. Rautio, "A new definition of characteristic impedance," in *IEEE MTT-S Int. Microwave Symp. Dig.*, 1991, pp. 761–764.
- [3] F. Arndt and G. U. Paul, "The reflection definition of the characteristic impedance of microstrips," *IEEE Trans. Microwave Theory Tech.*, vol. MTT-27, pp. 724–731, Aug. 1979.
- [4] J. C. Rautio, "Experimental validation of electromagnetic software," *Int. J. Microwave Millimeter-Wave Computer-Aided Eng.*, vol. 1, no. 4, pp. 379–385, Oct. 1991.
- [5] —, "An ultra-high precision benchmark for validation of planar electromagnetic analyzes," *IEEE Trans. Microwave Theory Tech.*, vol. MTT-42, pp. 2046–2050, Nov. 1994.
- [6] —, "An investigation of an error cancellation mechanism with respect to subsectional electromagnetic analysis validation," *Int. J. Microwave Millimeter-Wave Computer-Aided Eng.*, vol. 6, no. 6, pp. 430–435, Nov. 1996.
- [7] —, *The Evaluation of Electromagnetic Software*. Liverpool, NY: Sonnet Software, 1996.
- [8] E. H. Lenzing and J. C. Rautio, "A model for discretization error in electromagnetic analysis of capacitors," *IEEE Trans. Microwave Theory Tech.*, vol. MTT-46, pp. 162–166, Feb. 1998.
- [9] W. J. Getsinger, "Measurement and modeling of the apparent characteristic impedance of microstrip," *IEEE Trans. Microwave Theory Tech.*, vol. MTT-31, pp. 624–632, Aug. 1983.

#### Authors' Reply

Lei Zhu and Ke Wu

Rautio's comments touch down on some interesting and fundamental issues in connection with the longtime-disputed definition of characteristic impedance. In this paper, our attention will be focused on the evaluation issue of two error sources, namely, *port discontinuity* and *mesh size/number*, which are probably the most important factors contributing to the stability and accuracy problems of characteristic impedance of a microstrip line when the de-embedding procedure is implemented in a three-dimensional (3-D) method-of-moments<sup>1</sup> [1] (MoM) scheme. In [1], Rautio proposed the port discontinuity as a lumped shunt capacitance. In [2], it has been confirmed that this model is valid only at very low frequency and it should be expressed in terms of a distributed circuit network. This is in particular vital at high frequency or for electrically small structures.

Manuscript received September 23, 1998; revised October 1, 1998.

The authors are with Poly-Grames Research Center, Departement de Génie Electrique et de Génie Informatique, École Polytechnique de Montréal, Montréal, P.Q., Canada H3C 3A7.

Publisher Item Identifier S 0018-9480(99)00397-X.

<sup>1</sup>L. Zhu and K. Wu, *IEEE Microwave Guided Wave Lett.*, vol. 4, no. 2, pp. 87–89, Feb. 1998.

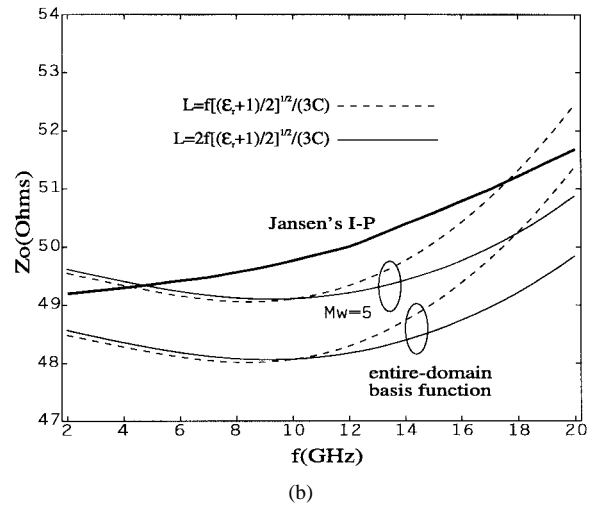
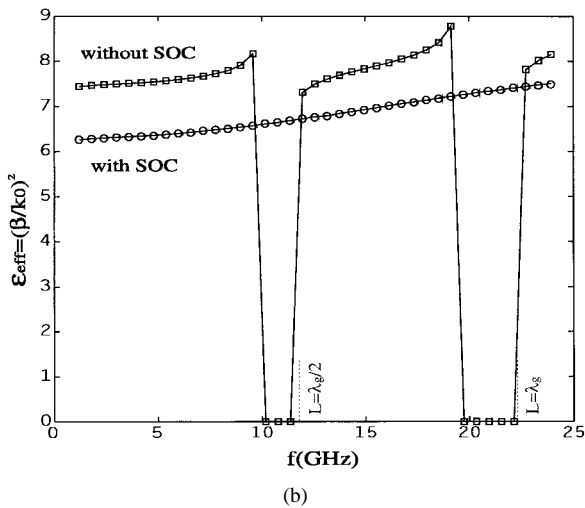
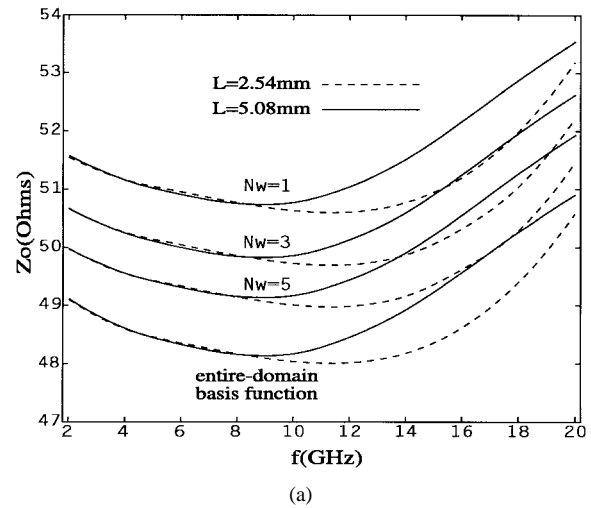
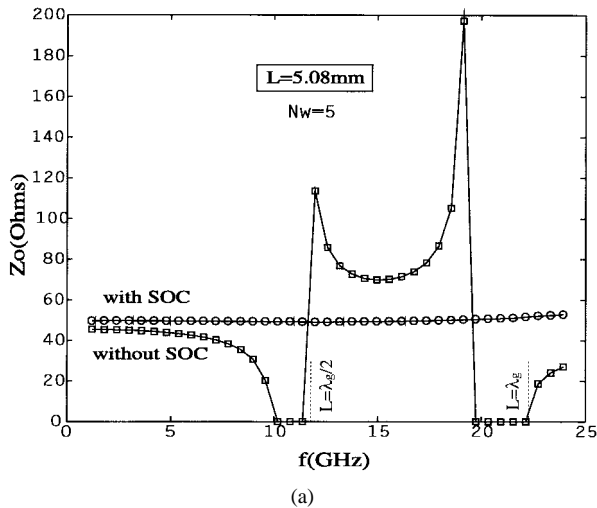


Fig. 1. Calculated characteristic impedance ( $Z_0$ ) and effective dielectric constant ( $\epsilon_{\text{eff}}$ ) versus frequency, which are de-embedded from the 3-D MoM modeling of a finite microstrip line with/without applying the SOC scheme. (a) Characteristic impedance  $Z_0$ . (b) Effective dielectric constant  $\epsilon_{\text{eff}}$ .

Fig. 2. Convergence behaviors of the calculated characteristic impedance against the mesh number  $N_w$  along the strip width and the finite physical/electrical length  $L$  of a microstrip line. (a) In the case of fixed physical length. (b) In the case of fixed electrical length.

From our modeling results, compiled from a large number of planar structures, we have developed a knowledge on the issue of how the port discontinuity affects the de-embedded parameters of a planar circuit. When an *electrically large* circuit is considered, the circuit parameter of such a port discontinuity is much smaller than those of the circuit under modeling. This error source causes a slight shift in frequency and/or a subtle change in magnitude for the parameters. In contrast, this error source usually leads to the instability and incorrectness of the de-embedded parameters for an *electrically small* circuit. The three possibilities suggested in Rautio's comments may be understood in depth only if the two above-mentioned error sources are considered in parallel.

#### I. ERRORS DUE TO THE PORT DISCONTINUITY

To look into effects of the port discontinuity, we begin with the study of a uniform line with finite length (in this case,  $L = 5.08$  mm) with/without consideration of the port discontinuity. Our objective is to examine the three-dimensional (3-D) (physical length) method-of-moments (MoM) algorithm when applied to a two-dimensional (2-D) (unit-length) problem. Simulated results in this case can thus be formulated by an admittance ( $Y$ ) matrix for a number of cascaded line sections representing the entire line length (*electrically large*

problem). This matrix can then be converted into characteristic impedance  $Z_0$  (3-D definition) of the line representing circuit equivalence per unit of length of the uniform line (*electrically small* problem). The effective dielectric constant  $\epsilon_{\text{eff}}$  can also be obtained. It is found that the elements of the admittance matrix remain unchanged at low frequency; however, they exhibit first and second harmonic resonances around 11.6 and 22.2 GHz, respectively. Recently, we have developed a new numerical de-embedding technique called short-open calibration (SOC) in the MoM scheme, inspired from the thru-reflection line (TRL) calibration concept in measurements. This technique allows extracting the potential error terms in the calculations, thereby providing very accurate and stable results even in the case of an *electrically small* structure. The SOC technique was detailed in [3]. Unfortunately, this paper has not been published yet. Before and after the use of the SOC technique in the calculations, the observable difference between the two scenarios is a shift of resonant frequency: 9.9 to 11.6 GHz and 21.8 to 22.2 GHz. In fact, it can be qualitatively explained by an equivalent-circuit model of the port discontinuity, as discussed in [2].

On the basis of Fig. 1(a) and (b),  $Z_0$  and  $\epsilon_{\text{eff}}$  are found to be smooth and stable with frequency once our SOC technique is applied in the 3-D MoM algorithm. Otherwise, those results appear to be

strongly affected by resonances as the frequency increases beyond the proximity of first resonant frequency. Obviously, there exist some harmful nonphysical values of  $Z_0$  and  $\varepsilon_{\text{eff}} (< 0)$  around the two resonant frequencies caused by  $|Y_{11}| > |Y_{21}|$ . Nevertheless, the results are relatively smooth and stable over low-frequency range and they converge toward those obtained with the SOC scheme. This confirms that the port discontinuity can effectively be perceived as a simple shunt capacitance, as proposed by Rautio in [1]. As shown in Tables I and II of Rautio's comments, the frequency was used to be lower than that representing the half-wavelength resonance, namely, 11.6 GHz for  $L = 5.08$  mm and 22.2 GHz for  $L = 2.54$  mm. Interestingly, the error percentage with the two different  $L$ 's is rapidly increased to 1.181% and 5.918% at 10 and 20 GHz, respectively, in Rautio's comments.

## II. ERRORS DUE TO THE MESH SIZE/NUMBER

Following the suggestion made in Rautio's comments, we would like to discuss the influence of the error source caused by the choice of a different mesh size/number along the transverse and longitudinal directions of a microstrip line. To showcase the convergence with respect to the strip width, the transverse current over the strip in the MoM algorithm can effectively be expressed in terms of the subdomain pulse (constant) basis functions or entire-domain basis functions involving the edge singularities. In parallel, the longitudinal current can be expanded as a summation of the well-documented subdomain sine/cosine basis functions.

Fig. 2(a) shows the frequency-dependent characteristic impedance  $Z_0$ , which is de-embedded by applying our SOC technique in the modeling of uniform lines  $L = 2.54$  mm and  $L = 5.08$  mm as used in Rautio's comments. As the mesh number  $N_w$  increases, the curve shape of frequency response remains almost the same and its value gradually falls toward the results generated by using the entire-domain basis functions. The error percentage for  $N_w = 5$  is close to 2.0% over the entire frequency range. As compared with our original results in the above paper<sup>1</sup>,  $Z_0$  exhibits a strong negative slope over 2–8 GHz, which can be attributed to the significant reduction in line length ( $L = 25.42$  mm in the above paper<sup>1</sup>). We observe that the error in relation to the longitudinal direction is mainly generated by

the line length  $L$  and, basically, it is irrelevant to the mesh number for a fixed  $L$ . The error percentage is substantiated by about 0.2% as the mesh size  $\Delta L$  is selected from 0.127 to 0.508 mm. The error source of  $L$  roughly indicates an incremental change of 2.0% around 16 GHz (high-frequency range), as described in Fig. 2(a), and it is expected to go beyond 3.5% if  $L = 10.16$  mm.

Fig. 2(b) shows our calculated results against that of Jansen's current–power definition on the assumption of two sets of fixed electrical lengths governed by  $L = f[(\varepsilon_r + 1)/2]^{1/2}/(3C)$  and  $L = 2f[(\varepsilon_r + 1)/2]^{1/2}/(3C)$ , in which  $C$  is the speed of light. It can be seen that  $Z_0$  still appears as some nonmonotonous dispersion with frequency, but its large variation is visibly reduced. As the electrical length at low frequency is extended,  $Z_0$  tends to slightly fall down with reference to the results plotted in Fig. 2(a). As a matter of fact, such a line extension can avoid the intercoupling between the input and output ports, and also the current profile can be more accurately modeled along the longitudinal direction. As frequency increases,  $Z_0$  is prone to gradually increase, similar to Fig. 2(a). This phenomenon may be attributed to the subtle influence of high-order modes appearing at high frequency, excited by the field launchers at the input/output ports.

In conclusion, it is our belief that the largest error in the de-embedding of  $Z_0$  on the basis of the 3-D modeling is essentially caused by the physical/electrical length  $L$  of a finite line. With the help of our proposed SOC scheme, we will be able to extract the error terms and generate accurate and stable results with the MoM field-based algorithms. As pointed out by Rautio, it is possible to use a consistent and standard 3-D definition of characteristic impedance for numerical analysis and experimental realization.

## REFERENCES

- [1] J. C. Rautio, "A new definition of characteristic impedance," in *IEEE MTT-S Int. Microwave Symp. Dig.*, 1991, pp. 761–764.
- [2] L. Zhu and K. Wu, "Network equivalence of port discontinuity related to source plane in a deterministic 3-D method of moments," *IEEE Microwave Guided Wave Lett.*, vol. 4, no. 3, pp. 130–132, Mar. 1998.
- [3] —, "Unified equivalent circuit model of planar discontinuities suitable for field theory-based CAD and optimization of M(H)MIC's," *IEEE Trans. Microwave Theory Tech.*, to be published.